Calcium Binding to Calmodulin Mutants Having Domain-Specific Effects on the Regulation of Ion Channels†

Wendy S. VanScyoc, Rhonda A. Newman, Brenda R. Sorensen, and Madeline A. Shea*

Department of Biochemistry, Roy J. and Lucille A. Carver College of Medicine, University of Iowa, Iowa City, Iowa 52242-1109

Received June 7, 2006; Revised Manuscript Received September 1, 2006

ABSTRACT: Calmodulin (CaM) is an essential, eukaryotic protein comprised of two highly homologous domains (N and C). CaM binds four calcium ions cooperatively, regulating a wide array of target proteins. A genetic screen of *Paramecia* by Kung [Kung, C. et al. (1992) *Cell Calcium 13,* 413−425] demonstrated that the domains of CaM have separable physiological roles: "under-reactive" mutations affecting calcium-dependent sodium currents mapped to the N-domain, while "over-reactive" mutations affecting calcium-dependent potassium currents localized to the C-domain of CaM. To determine whether and how these mutations affected intrinsic calcium-binding properties of CaM domains, phenylalanine fluorescence was used to monitor calcium binding to sites I and II (N-domain) and tyrosine fluorescence was used to monitor sites III and IV (C-domain). To explore interdomain interactions, binding properties of each full-length mutant were compared to those of its corresponding domain fragments. The calcium-binding properties of six under-reactive mutants (V35I/D50N, G40E, G40E/D50N, D50G, E54K, and G59S) and one over-reactive mutant (M145V) were indistinguishable from those of wild-type CaM, despite their deleterious physiological effects on ion-channel regulation. Four over-reactive mutants (D95G, S101F, E104K, and H135R) significantly decreased the calcium affinity of the C-domain. Of these, one (E104K) also *increased* the calcium affinity of the N-domain, demonstrating that the magnitude and direction of wild-type interdomain coupling had been perturbed. This suggests that, while some of these mutations alter calcium-binding directly, others probably alter CaM-channel association or calcium-triggered conformational change in the context of a ternary complex with the affected ion channel.

Calmodulin (CaM;[1] Figure 1) is comprised of two highly homologous domains that appear to have arisen from two successive gene-duplication events. Sequence alignment indicates that the four calcium-binding sites (I and II in the N-domain and III and IV in the C-domain, Figure 1) are very similar; of the 12 amino acids in each site, positions 1(D), 3(D), 4(G), 6(G), and 12(E) are identical in all four. Although these sites in CaM are in homologous helix−loop−helix motifs or EF-hands, calcium binding to the domains is sequential: sites III and IV in the C-domain are nearly 100% saturated before saturation of sites I and II in the N-domain reaches a few percentages (*1*, *2*).

Calcium binding to CaM causes major structural changes, including exposure of a hydrophobic cleft in each domain (*3*); these surfaces mediate protein−protein interactions that enable CaM to function as a member of many calcium-dependent signal transduction cascades. The level of calcium saturation required for the interaction with targets can vary. A high-resolution structure of apo (calcium-depleted) CaM associated with a long peptide fragment of a calcium-activated small conductance potassium (SK) channel (*4*) and two crystallographic studies of half-saturated CaM [$(Ca^{2+})_2$-CaM] associated with targets (*5*, *6*) demonstrate that calcium saturation is not required for specific CaM−target interactions. Apo-CaM can bind to some targets with a higher affinity than calcium-saturated CaM [$(Ca^{2+})_4$-CaM] (*7*, *8*) and serves as an integral enzyme subunit (*9*) or ion-channel subunit (*10*) that is bound constitutively.

A comparison of the high-resolution structures of CaM bound to its targets in these different ligation states illustrates the broad potential for molecular plasticity that was envisioned when models of co-complexes of CaM bound to a peptide from MLCK (*11*, *12*) and CaMKII (*13*) showed that "the central helix" of CaM could bend to accommodate a target protein. While the CaM−target complexes with only 2 equiv of calcium demonstrate separable roles of the two homologous domains in target recognition and activation, this principle was originally discovered via a genetic screen of *Paramecium tetraurelia* that identified two classes of deviant chemotactic phenotypes and defective ion-channel regulation (*14*). Unexpectedly, both classes of mutants were linked to mutations in CaM (not to the sequences of the

† These studies were supported by a University of Iowa Center for Biocatalysis and Bioprocessing Graduate Fellowship to W.S.V., a University of Iowa Center for Biocatalaysis and Bioprocessing NIH Biotechnology Training grant (NIH T32 GM08365-13) to R.A.N., and a grant to M.A.S. from the National Institutes of Health (RO1 GM 57001).

* To whom correspondence should be addressed. Telephone: (319) 335-7885. Fax: (319) 335-9570. E-mail: madeline-shea@uiowa.edu.

[1] Abbreviations: CaM, calmodulin; CSU, Contacts of Structural Units; EGTA, ethylene glycol bis(aminoethyl ether)-*N*,*N*,*N*′,*N*′-tetraacetic acid; HEPES, *N*-2-hydroxyethylpiperazine-*N*′-2-ethanesulfonic acid; NTA, nitrilotriacetic acid; PCaM, *Paramecium* calmodulin; $PCaM_{1-80}$, N-domain fragment of PCaM terminating at residue 80; $PCaM_{76-148}$, C-domain fragment of PCaM starting at residue 76; $PCaM_{1-148}$, full-length PCaM; PDB, Protein Data Bank; Phe, phenylalanine; Tyr, tyrosine.

10.1021/bi061134d CCC: $33.50
Published on Web 11/09/2006

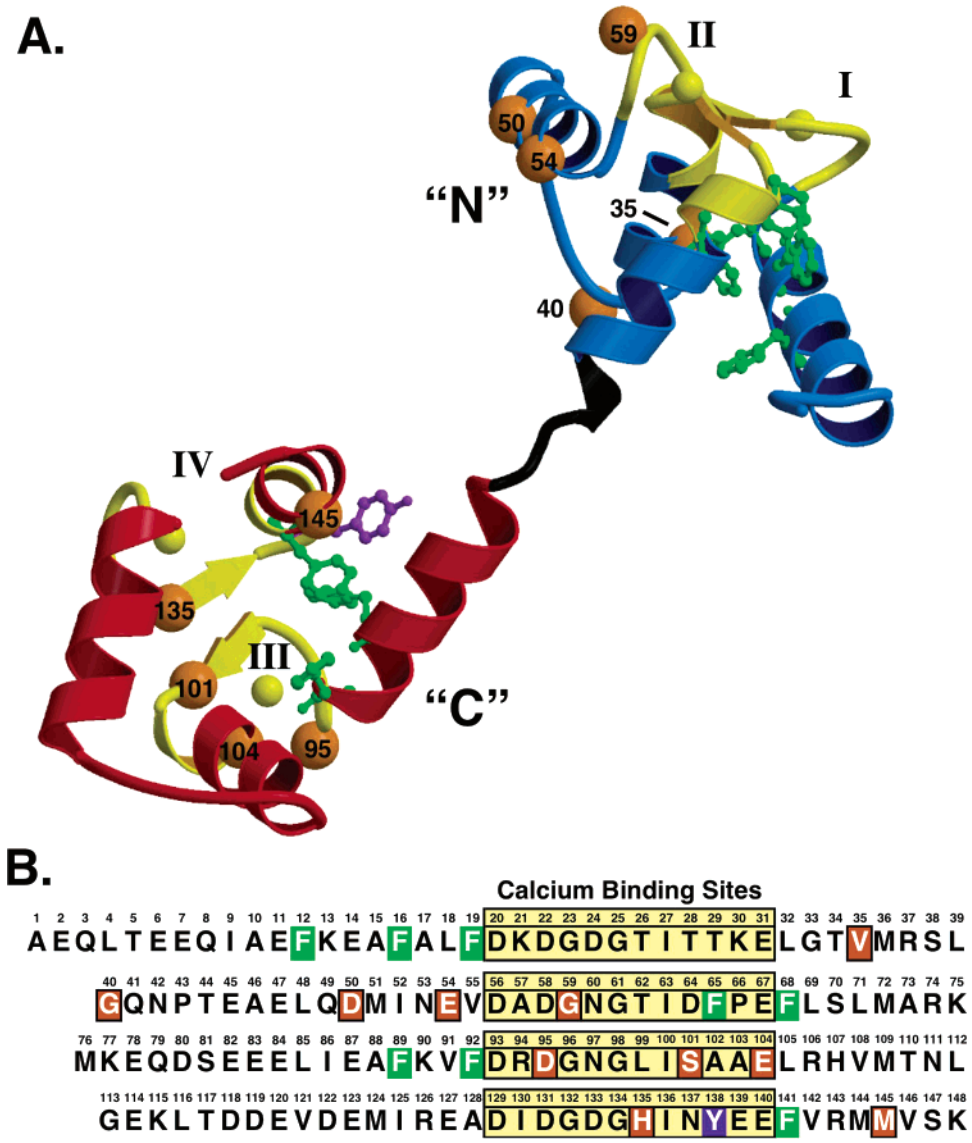

FIGURE 1: Calcium-saturated PCaM. (A) Ribbon diagram of calcium-saturated PCaM [PDB 1OSA (*52*)] created with MOLSCRIPT (*53*) and RASTER3D (*54*). Backbone atoms of residues in calcium-binding loops (I, II, III, and IV) and calcium ions are yellow; positions of mutations are indicated by orange spheres. Fluorescent residues Phe (green) and Tyr (violet) are shown in a ball-and-stick representation. (B) Sequence alignment of the four calcium-binding sites in PCaM. Highlighted are positions of mutations (orange), Phe residues (green), and the single Tyr residue (violet) in wild-type PCaM.

calcium-dependent ion channel per se), and each phenotype was mapped to a specific domain of CaM.

Mutations in the N-domain of *Paramecium* CaM (PCaM) caused *Paramecia* to under-react to various stimuli; they showed little or no reversal in swimming direction in response to stimuli compared to wild-type *Paramecia*. These mutations also caused defective calcium-activated sodium currents. As shown in Figure 1, all but one of these mutations is *between* sites I and II (the exception is G59S in site II). This region is known to change conformation when calcium binds to the C-domain (*15*−*17*), and nearby methionine residues (M36 and M51) contribute to the hydrophobic clefts of CaM that have an important role in calcium-dependent molecular recognition of target proteins (*18*, *19*).

In contrast to the mutations found in the N-domain of PCaM, Kung and co-workers found that mutations in the C-domain of PCaM (Figure 1) caused an over-reactive phenotype, whereby a negative stimulus caused *Paramecia* to swim in the reverse direction longer than observed for wild-type *Paramecia* (i.e., avoidance behavior persisted longer than normal). These C-domain mutations also caused defective calcium-activated potassium currents. All but one of these over-reactive mutations were *within* sites III and IV and were expected to disrupt calcium binding to the C-domain. The outlying mutation M145V was located in the terminal helix of CaM (following site IV) and disrupted one of two occurrences of vicinal methionine residues in CaM (see Figure 1).

Although the CaM-binding domains of the affected *Paramecium* ion channels have not yet been identified, an essential first step in understanding the molecular basis for defective calcium-dependent signaling by these viable mutants is to characterize their effects on the intrinsic calcium-binding properties of both domains of PCaM. Presumably, differences in the ability of a mutant sequence to bind calcium at concentrations that would be sufficient for activating wild-type PCaM would contribute to differences in the ability of that mutant to bind to and regulate calcium-dependent

ion channels. CaM is in equilibrium between the free and channel-bound forms. Therefore, the intrinsic calcium-binding affinity of each PCaM mutant, as well as its calcium affinity when bound to channels or other targets, will be of interest in understanding the biological effects of these mutants.

Equilibrium constants for calcium binding to full-length PCaM ($PCaM_{1-148}$) were determined directly by monitoring the decrease in intrinsic phenylalanine (Phe) fluorescence (which selectively reports on the occupancy of the pair of sites in the N-domain) and the increase in intrinisic tyrosine (Tyr) fluorescence (which selectively reports on the occupancy of the pair of sites in the C-domain) of $PCaM_{1-148}$ (*20*). The position of these native fluorophores is illustrated in Figure 1. Results were compared to those obtained for calcium binding to the same sites in isolated N-domain ($PCaM_{1-80}$) or C-domain ($PCaM_{76-148}$) fragments to investigate whether the mutations perturbed normal interdomain interactions in $PCaM_{1-148}$.

The calcium-binding titrations in this study were conducted under physiological magnesium conditions and showed that the under-reactive mutations (all located in the N-domain of PCaM) and M145V, the single over-reactive mutation that is outside of sites III and IV (in the C-domain of PCaM), did not alter the calcium-binding properties of PCaM. In contrast, all four of the over-reactive mutations that are within sites III or IV showed a decrease in affinity for calcium binding to sites III and IV in $PCaM_{1-148}$ and $PCaM_{76-148}$, with the greatest effect observed for E104K, which abolished binding to site III. A mutation in site III (D95G) seemed to abolish the cooperativity of binding calcium to sites III and IV in $PCaM_{1-148}$ and $PCaM_{76-148}$. The mutations D95G, S101F, and H135R in the C-domain had no effect on calcium binding to the N-domain (their effects were local). However, the mutation E104K, which altered the bidentate glutamate at position 12 in site III, had the most deleterious effect on the C-domain and also increased the calcium-binding affinity of sites I and II in the N-domain, perturbing interdomain interactions. These results provide evidence for the allosteric regulation of domain differences in calcium affinity.

This analysis of calcium binding and calcium-induced switching suggests two distinct models for the molecular determinants of domain-specific regulation of calcium-dependent ion channels by CaM. It suggests that most over-reactive mutants lower intrinsic calcium binding directly and thereby increase the level of calcium required to allow PCaM to associate with and close a potassium channel during a cellular influx of calcium. In contrast, the under-reactive mutants probably act by altering the association constant of PCaM for a target or changing the calcium-triggered conformational change in the context of a ternary complex with the affected sodium ion channel.

MATERIALS AND METHODS

Chemicals. All chemicals were reagent-grade.

Overexpression and Purification of CaM. Original vectors for *Paramecium* wild-type and mutant $PCaM_{1-148}$ genes were a gift from C. Kung, University of Wisconsin—Madison. The DNA encoding full-length $PCaM_{1-148}$ sequences (the wild type and the 11 PCaM mutants: V35I/D50N, G40E, G40E/D50N, D50G, E54K, G59S, D95G, S101F, E104K, H135R, and M145V); the corresponding N-domain fragments ($PCaM_{1-80}$) of the wild-type protein and mutants V35I/D50N, G40E, G40E/D50N, D50G, E54K, G59S; and C-domain fragments ($PCaM_{76-148}$) of the wild-type protein and mutants D95G, S101F, E104K, H135R, and M145V were cloned into the bacterial overexpression vector pT7-7 (*21*, *22*) using standard techniques (*17*) and overexpressed in *E. coli* Lys-S cells (U.S. Biochemicals, Cleveland, OH) as described previously (*15*). Proteins were purified as described by Putkey et al. (*23*); some protein preparations underwent an additional 10 min of incubation at 80 °C in saturating calcium (10 mM $CaCl_2$) to precipitate any remaining contaminating proteins. The recombinant proteins were 97−99% pure as judged by silver-stained SDS−PAGE and reversed-phase HPLC. Sequencing of plasmids was conducted by the DNA Facility, and amino acid analysis of proteins was conducted by the Molecular Analysis Facility, both at the University of Iowa Carver College of Medicine.

Equilibrium Calcium Titrations. Titrations were conducted in a thermally jacketed quartz cuvette and monitored using 8 nm bandpasses on an SLM 4800 (SLM Instruments, Inc., Champaign-Urbana, IL) or 4 nm bandpasses on a PTI-QM4 spectrofluorometer (Photon Technology International, Birmingham, NJ); both were equipped with a xenon short arc lamp (Ushio, Inc.). PCaM samples [6 μM in 50 mM *N*-2-hydroxyethylpiperazine-*N*′-2-ethanesulfonic acid (HEPES), 100 mM KCl, 1 mM $MgCl_2$, 0.05 mM ethylene glycol bis-(aminoethyl ether)-*N*,*N*,*N*′,*N*′-tetraacetic acid (EGTA), and 5 mM nitrilotriacetic acid (NTA) buffer at pH 7.4 and 22 °C] were titrated with a concentrated calcium solution (50 mM to 1 M $CaCl_2$ in the same buffer) using a microburet outfitted with a Hamilton syringe. Note the buffer contained 1 mM $MgCl_2$ total, but the calculated free concentration of Mg^{2+} was lower (~150 μM) at the start of the calcium titration and increased as the calcium concentration increased.

Calcium binding to sites I and II was monitored by observing calcium-dependent changes in the steady-state fluorescence intensity of the five Phe residues in the N-domain (λ_{ex} of 250 nm and λ_{em} of 280 nm), and binding to sites III and IV was monitored by observing calcium-dependent changes in the steady-state fluorescence intensity of the single Tyr residue in the C-domain (λ_{ex} of 277 nm and λ_{em} of 320 nm) as developed for mammalian CaM (*20*). Calcium titrations of $PCaM_{1-148}$ under stoichiometric conditions indicated that, like mammalian CaM, the decrease in Phe fluorescence of $PCaM_{1-148}$ was linearly proportional to the calcium occupancy of sites I and II and the increase in Tyr fluorescence was linearly proportional to the calcium occupancy of sites III and IV (data not shown) (*24*). Although the PCaM mutant domain fragments each contained only one pair of sites, both sets of wavelengths were monitored to ascertain that they retained the properties of wild-type fragments.

The fluorescent dye Oregon Green 488 BAPTA-5N (0.1 μM; Molecular Probes, Eugene, OR) was used as an indicator of free calcium concentration (see eq 1)

$$[\text{calcium}]_{\text{free}} = K_d \frac{f_{[\text{high}]} - f_{[X]}}{f_{[X]} - f_{[\text{low}]}} \quad (1)$$

where $f_{[high]}$ is the fluorescent intensity of Oregon Green at the high plateau (high calcium), $f_{[low]}$ is the fluorescent intensity at the low plateau (calcium depleted), and $f_{[X]}$ is

the intensity of the indicator dye after each addition of calcium. The K_d of calcium binding to Oregon Green was determined experimentally to be 34.24 μM in 50 mM HEPES, 100 mM KCl, and 1 mM $MgCl_2$ at pH 7.4 and 22 °C (*25*). Calcium titrations of wild-type PCaM and each mutant sequence were repeated 3−9 times. Representative titrations are shown in Figures 2−4 and 6.

Stoichiometric Calcium Titrations. Wild-type $PCaM_{1-148}$ binds 4 equiv of calcium, and each domain fragment ($PCaM_{1-80}$ and $PCaM_{76-148}$) binds 2 equiv of calcium. For each protein that showed a decrease in the median calcium concentration of equilibrium titrations relative to the behavior of the corresponding wild-type sequence, the number of calcium ions bound at saturation was determined by monitoring changes in steady-state fluorescence throughout stoichiometric calcium titrations of highly concentrated (60−150 μM) solutions of PCaM (data not shown). All of the mutants except E104K showed a stoichiometry of binding corresponding to 4 calcium per $PCaM_{1-148}$ and 2 calcium per $PCaM_{1-80}$ or $PCaM_{76-148}$. Stoichiometric titrations of E104K $PCaM_{76-148}$ and E104K $PCaM_{1-148}$ showed that the C-domain of this mutant bound only 1 calcium ion, consistent with previous stoichiometric calcium titrations of E104Q *Drosophila* CaM monitored by 1D proton nuclear magnetic resonance (NMR) (*26*). The N-domain of E104K $PCaM_{1-148}$ has a wild-type sequence; it bound 2 equiv of calcium, for a total of 3.

Analysis of Free Energies of Binding. Each domain of CaM may be considered as a two-site macromolecule described by the linkage diagram below (*27*).

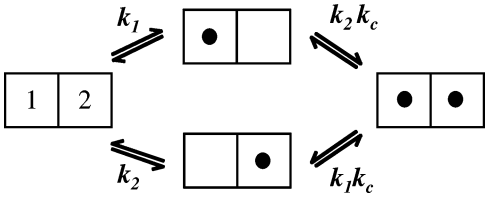

Free energies of calcium binding to sites I and II or to sites III and IV were determined by fitting the data to a model-independent two-site binding function (eq 2a) originally described by Adiar (*28*). The nomenclature in the expression for fractional saturation has been used in prior publications from this laboratory (*16*, *17*, *29*) and many others (*30*−*34*)

$$\bar{Y}_{total} = \bar{Y}_2 = \frac{K_1[X] + 2K_2[X]^2}{2(1 + K_1[X] + K_2[X]^2)} \quad (2a)$$

where [X] represents the free calcium concentration and K_1 is the sum of intrinsic microscopic equilibrium constants ($k_1 + k_2$) for two sites: either sites I and II in the N-domain or sites III and IV in the C-domain. The second macroscopic equilibrium constant (K_2) is the product ($k_1k_2k_c$) of the intrinsic constants with the cooperativity constant, k_c. The parameters ΔG_1 and ΔG_2 are macroscopic binding free energies with ΔG_i equal to $-RT \ln K_i$. In the case of a two-site domain having only one functioning binding site, the expression for fractional saturation reduces to

$$\bar{Y}_{total} = \bar{Y}_1 = \frac{k_1[X]}{(1 + k_1[X])} \quad (2b)$$

To account for normal variations in the values of the high and low endpoints of fluorescence intensity in each titration (these are a function of slight differences in the starting concentration of CaM, age of the lamp, etc.), the function [f(X)] used for nonlinear least-squares analysis of the calcium-dependent change in fluorescence intensity is given by

$$f(X) = Y_{[X]low} + \bar{Y} \cdot span \quad (3)$$

where $\bar{Y}$ refers to the average fractional saturation as described by eq 2a or 2b, $Y_{[X]low}$ is the fluorescence intensity at the lowest calcium concentration, and *span* is the difference between the fluorescence intensity signal at high and low ligand concentrations (*15*). Note that the value of the parameter *span* is negative for the calcium-dependent decrease in intensity of Phe fluorescence resulting from calcium binding to sites I and II and positive for the calcium-dependent increase in intensity of Tyr fluorescence resulting from calcium binding to sites III and IV. Values for all parameters were fit simultaneously. Average free energies and standard deviations based on individual nonlinear least-squares analysis of 3−9 replicate titrations are reported in Tables 1 and 2.

The free energy of cooperativity between the sites in each domain may be estimated from the macroscopic equilibrium constants only by assuming that calcium binds with equal intrinsic affinity to the paired sites in a domain. The value of $\Delta G_c(-RT \ln(k_c))$ is given by the expression in eq 4

$$\Delta G_c = \Delta G_2 - 2\Delta G_1 - RT \ln(4) \quad (4)$$

If the values of k_1 and k_2 are not equal, using this equation to estimate ΔG_c provides a lower limit (underestimate) for the degree of cooperative interaction between the sites (see ref *15* for a discussion).

Perturbations of Fluorescence Intensities Caused by a Mutation. The calcium-dependent decrease in Phe fluorescence intensity of wild-type $PCaM_{1-148}$ reports exclusively on calcium binding to the N-domain, while the increasing Tyr fluorescence reports exclusively on calcium binding to the C-domain (*20*). However, the validity of this interpretation for the mutants had to be tested experimentally. None of the mutations in the N-domain changed the content of aromatic amino acids. Analysis of stoichiometric titrations showed that the calcium-induced changes in steady-state fluorescence intensity were linearly proportional to occupancy, as observed for wild-type PCaM (data not shown). However, the mutation S101F introduced an additional Phe residue into the C-domain within site III. It was necessary to determine whether this residue would contribute a calcium-dependent change to the net fluorescence intensity measured for PCaM or whether it would be quenched in the same manner as the other three Phe residues are in the wild-type sequence. Furthermore, it was necessary to determine whether other over-reactive mutations in the C-domain might perturb the conformation of CaM in a manner that would change the interpretation of the Phe signal as representing calcium binding only to sites I and II. This was addressed by determining whether the C-domain fragment ($PCaM_{76-148}$) of each mutant PCaM displayed a calcium-dependent change

Table 1: Free Energies of Calcium Binding to N-Domain Sites I and II

protein	length	ΔG_1[a]	ΔG_2[a]	$\Delta\Delta G_2$[b]
wild-type	1−148	−6.09 ± 0.33	−12.26 ± 0.08	n/a
	1−80[c]	−5.80 ± 0.31	−12.13 ± 0.10	n/a
V35I/D50N	1−148	−6.52 ± 0.09	−12.37 ± 0.09	−0.11
	1−80	−5.86 ± 0.17	−12.07 ± 0.11	0.06
G40E	1−148	−5.75 ± 0.37	−12.51 ± 0.05	−0.25
	1−80	−5.97 ± 0.13	−12.49 ± 0.01	−0.36
G40E/D50N	1−148	−5.54 ± 0.32	−12.67 ± 0.08	−0.41
	1−80	−6.08 ± 0.05	−12.71 ± 0.02	−0.58
D50G	1−148	−6.19 ± 0.13	−12.40 ± 0.06	−0.14
	1−80	−5.81 ± 0.14	−12.20 ± 0.03	−0.07
E54K	1−148	−6.28 ± 0.13	−12.31 ± 0.09	0.05
	1−80	−5.75 ± 0.10	−12.03 ± 0.04	0.10
G59S	1−148	−6.24 ± 0.15	−12.32 ± 0.09	0.06
	1−80	−5.71 ± 0.17	−12.13 ± 0.06	0.00
D95G	1−148	−6.26 ± 0.11	−12.34 ± 0.02	−0.08
S101F[d]	1−148	−5.81 ± 0.10	−12.04 ± 0.05	0.22
E104K	1−148	−6.59 ± 0.02	−13.08 ± 0.06	−0.82
H135R	1−148	−6.07 ± 0.20	−12.41 ± 0.09	−0.15
M145V	1−148	−6.47 ± 0.08	−12.58 ± 0.05	−0.32

[a] Gibbs free energies (in kcal/mol; 1 kcal = 4.184 kJ). Values and errors represent averages and standard deviations between 3 and 9 trials. The square root of the variance ranged from 0.010 to 0.057. [b] $\Delta\Delta G_2 = \Delta G_2$(mutant) − ΔG_2(wild-type) (in kcal/mol). [c] Taken from ref *25*. [d] Gibbs free energy resolved from the decrease in Phe fluorescence for S101F $PCaM_{1-148}$ shown in Figure 6 that is represented by a 22.5% contribution from the C-domain and a 77.5% contribution from the N-domain of S101F $PCaM_{1-148}$ (see the Results).

Table 2: Free Energies of Calcium Binding to C-Domain Sites III and IV

protein	length	ΔG_1[a]	ΔG_2[a]	$\Delta\Delta G_2$[b]
wild-type	1−148	−7.76 ± 0.20	−15.92 ± 0.12	n/a
	76−148	−6.45 ± 0.50	−15.49 ± 0.13	n/a
V35I/D50N	1−148	−7.76 ± 0.30	−15.82 ± 0.08	0.10
G40E	1−148	−7.35 ± 0.63	−16.11 ± 0.08	−0.19
G40E/D50N	1−148	−7.80 ± 0.10	−16.07 ± 0.06	−0.15
D50G	1−148	−7.61 ± 0.08	−16.06 ± 0.05	−0.14
E54K	1−148	−7.45 ± 0.25	−15.60 ± 0.08	0.32
G59S	1−148	−8.00 ± 0.26	−16.24 ± 0.08	−0.32
D95G	1−148	−7.07 ± 0.04	−13.02 ± 0.09	2.90
	76−148	−6.65 ± 0.07	−12.58 ± 0.09	2.91
S101F	1−148	−6.67 ± 0.19	−13.62 ± 0.09	2.30
	76−148	−5.68 ± 0.12	−13.17 ± 0.02	2.32
H135R	1−148	−6.41 ± 0.11	−13.79 ± 0.08	2.13
	76−148	−5.35 ± 0.75	−13.46 ± 0.09	2.03
M145V	1−148	−7.00 ± 0.90	−15.59 ± 0.07	0.33
	76−148	−6.52 ± 0.33	−15.24 ± 0.14	0.25
E104K[c]	1−148	−6.78 ± 0.02		
	76−148	−6.54 ± 0.04		

[a] Gibbs free energies (in kcal/mol; 1 kcal = 4.184 kJ) are described (eq 2a). Free energies and errors represent averages and standard deviations between 3 and 9 trials. The square root of the variance ranged from 0.006 to 0.046. [b] $\Delta\Delta G_2$ is the difference between ΔG_2 for mutants and wild-type CaM (in kcal/mol). [c] Stoichiometric calcium titrations of E104K$_{76-148}$ and E104K$_{1-148}$ indicated that this mutation abolishes the binding to site III (data not shown). Therefore, the Gibbs free energies reported for binding to the C-domain of this mutant were resolved from fitting to a single-site Adair function (eq 2b).

in intensity at 280 nm when excited at 250 nm (the same wavelength pair used to monitor calcium-dependent changes in Phe intensity of the N-domain).

Calcium titrations of the C-domain fragments ($PCaM_{76-148}$) of all over-reactive mutants showed that only S101F $PCaM_{76-148}$ exhibited a calcium-dependent change in the intensity of fluorescence emission at 280 nm. The observed decrease in fluorescence indicated that the change in the Phe fluorescence of S101F $PCaM_{1-148}$ included a component sensitive to calcium binding to the C-domain as well as calcium binding to the N-domain. To account for the spectroscopic contribution from calcium binding to the C-domain, the observed fluorescence intensity was fit to a sum of 2 two-site (Adair) binding equations, each having an amplitude representing the fraction of Phe fluorescence intensity coming from each domain. This is expressed in eq 5

$$\bar{Y}_{\text{total}} = f_N\bar{Y}_N + f_C\bar{Y}_C \quad (5)$$

where f_N represents the fraction of Phe fluorescence contributed by calcium binding to the N-domain, $\bar{Y}_N$ represents the fractional saturation of the N-domain, f_C represents the fraction of Phe fluorescence contributed by calcium binding to the C-domain, and $\bar{Y}_C$ represents the fractional saturation of the C-domain. The value for f_C was determined experimentally by performing titrations of S101F $PCaM_{76-148}$ using solution conditions and instrument settings identical to those of S101F $PCaM_{1-148}$ and comparing the absolute changes in intensity (values from three replicate experiments were averaged). The absolute change in the Phe intensity observed for S101F $PCaM_{76-148}$ alone was determined to be 22.5 ± 1.7% of that observed for S101F $PCaM_{1-148}$. Thus, the fractional contribution of the Phe residues in the N-domain was calculated as the complement ($1 - f_C$): 77.5%. This calculation assumes that the spectroscopic behavior of S101F $PCaM_{76-148}$ represents the behavior of that domain within S101F $PCaM_{1-148}$.

The titration data were fit to eq 6, which allows for variations in the initial fluorescence intensity ($Y_{[X]low}$) and *span* of the data

$$\text{signal} = f(X) = Y_{[X]low} + (f_N\bar{Y}_N + f_C\bar{Y}_C)\cdot span \quad (6)$$

The free energies of calcium binding to sites I and II (ΔG_1 and ΔG_2) in S101F $PCaM_{1-148}$ (see Table 1) were resolved by fixing f_C to the experimentally determined value of 22.5% and calculating $\bar{Y}_C$ using the values of free energies resolved from fitting the calcium-dependent change in Tyr fluorescence of S101F $PCaM_{1-148}$ to eq 2a (see Table 2).

Anti-cooperativity versus Unequal Affinity. For a macromolecule or domain that binds 2 mol of ligand, the expression for average fractional saturation (eq 2a) makes no assumption about the relative affinities of the two sites. However, analytically identical macroscopic binding isotherms may arise from two cases that are quite distinct in terms of microscopic energetics. Case "a", in which the sites have unequal intrinsic association constants ($k_1 \neq k_2$) and bind ligand independently ($k_c = 1$), may appear to be identical to case "b", in which sites have equal intrinsic association constants ($k_1 = k_2$) but anti-cooperative binding ($k_c < 1$). Distinguishing experimentally between cases "a" and "b" would require a method that could determine individual-site binding isotherms under equilibrium conditions (*27*). The steady-state fluorescence approaches applied in this study cannot do that; however, it is possible to calculate the maximum level of microscopic heterogeneity consistent with an experimentally determined macroscopic titration (i.e., one that gives the average degree of saturation) determined from calcium-dependent changes in fluorescent intensity.

Proteins for which the value of ΔG_c (eq 4) was close to 0 were candidates for those that bound calcium independently

and nonequivalently at two sites (i.e., according to case "a"). For these, the model-independent values of K_1 and K_2 were used to calculate microscopic equilibrium constants (k_1 and k_2) consistent with the titrations by setting the value of ΔG_c to 0 (i.e., $k_c = 1$) and calculating values of k_1 and k_2 using expressions in eqs 7 and 8

$$k_1 = \frac{K_1 + \sqrt{K_1^2 - 4K_2}}{2} \quad (7)$$

$$k_2 = \frac{K_2}{k_1} \quad (8)$$

This calculation provides a limit on the magnitude of the difference between intrinsic affinities of two sites that would be consistent with the experimental titration curve. The average fractional saturation for a molecule with no cooperativity between two sites is given by eq 9 and is equivalent to the average of two individual-site isotherms, each characterized by an intrinsic affinity, k_i

$$\bar{Y}_t = \frac{1}{2}(\bar{Y}_1 + \bar{Y}_2) = \frac{k_1[X]}{2(1 + k_1[X])} + \frac{k_2[X]}{2(1 + k_2[X])} \quad (9)$$

The value of ΔG_c for mutant D95G $PCaM_{1-148}$ was close to 0 and had the greatest deviation from the value for wild-type $PCaM_{1-148}$. Values of k_1 and k_2 consistent with k_c equal to 1 were calculated from the model-independent free energies, and simulations of the two non-identical individual-site isotherms ($\bar{Y}_1$ and $\bar{Y}_2$) were compared to the best-fit macroscopic isotherm for the C-domain as shown in Figure 6F.

RESULTS

Wild-Type PCaM. An equilibrium calcium titration of wild-type $PCaM_{1-148}$ is shown in Figure 2A. From analysis of the calcium-dependent decrease in fluorescence intensity of Phe (▲), the total free energy (ΔG_2) of calcium binding to sites I and II in wild-type $PCaM_{1-148}$ was determined to be -12.26 ± 0.08 kcal/mol (see Table 1). From analysis of the calcium-dependent increase in fluorescence intensity of Tyr (△), the total free energy of calcium occupancy of sites III and IV was determined to be -15.92 ± 0.12 kcal/mol (see Table 2). Values of free energies reported in Tables 1 and 2 indicate the average and standard deviation of nonlinear least-squares analysis of at least three discrete trials. For all of the titrations included in the analysis, the confidence intervals of the individual fits for total free energy (ΔG_2) were smaller than 0.10 kcal/mol. Solid curves show titrations simulated using the best-fit values for the data set shown.

The difference between the free energy of calcium binding to the C- and N-domain sites of $PCaM_{1-148}$ was -3.66 kcal/mol (a factor of 22 difference in K_{eq} per site at 22 °C). The lower limit of cooperative free energy (ΔG_c) between sites I and II was calculated to be -0.89 kcal/mol, and ΔG_c between sites III and IV was -1.21 kcal/mol. NMR studies of wild-type $PCaM_{1-148}$ showed that both sites in each domain filled simultaneously (*2*). This is consistent with the intrinsic association constants k_1 and k_2 being equal, although the intradomain cooperativity may mask subtle differences.

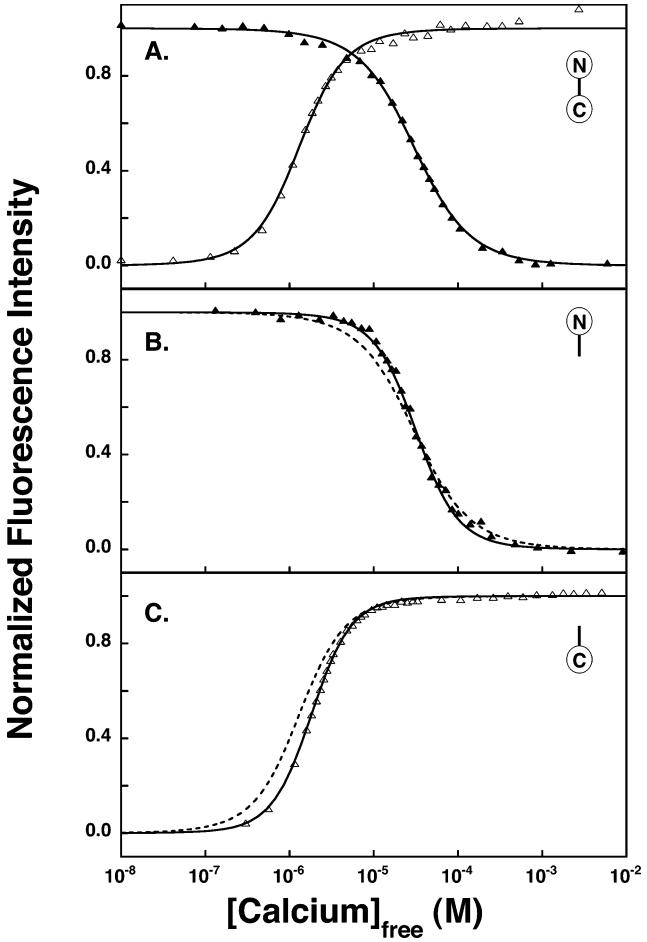

FIGURE 2: Calcium titration of wild-type PCaM monitored by Phe and Tyr fluorescence. The normalized fluorescence intensity [$(f - f_{min})/(f_{max} - f_{min})$] for Phe (▲) and Tyr (△) is shown as a function of free calcium for titrations conducted in 50 mM HEPES, 100 mM KCl, 1 mM $MgCl_2$, 50 μM EGTA, and 5 mM NTA at pH 7.4 and 22 °C. (A) Wild-type $PCaM_{1-148}$, (B) wild-type $PCaM_{1-80}$, and (C) wild-type $PCaM_{76-148}$. The solid black curve was simulated using the best-fit values resolved for the data set shown. Dashed curves indicate calcium binding to (B) sites I and II and (C) sites III and IV in wild-type $PCaM_{1-148}$ for a comparison to the corresponding domain fragment.

The energetics of calcium binding to the paired sites in $PCaM_{1-148}$ were compared to those of the same sites in the corresponding domain fragments. Figure 2B shows a representative titration of sites I and II in an isolated N-domain fragment ($PCaM_{1-80}$); filled triangles show the normalized values of the observed calcium-dependent decrease in Phe fluorescence. The average total free energy was -12.13 ± 0.1 kcal/mol; the solid curve was simulated using the best-fit values resolved from the data set shown. For a comparison, a titration of sites I and II in $PCaM_{1-148}$ is shown as the dashed curve. The small decrease in calcium affinity of $PCaM_{1-80}$ relative to $PCaM_{1-148}$ ($\Delta\Delta G_2$ of 0.13 kcal/mol) was close to the standard deviations (0.08 and 0.10) of the determinations of ΔG_2 for calcium binding to the N-domain sites I and II in $PCaM_{1-148}$ and $PCaM_{1-80}$.

Figure 2C shows a titration of sites III and IV in the isolated C-domain fragment ($PCaM_{76-148}$); open triangles represent normalized values of the observed calcium-dependent increase in Tyr fluorescence. The average total free energy was -15.49 ± 0.13 kcal/mol; the solid curve

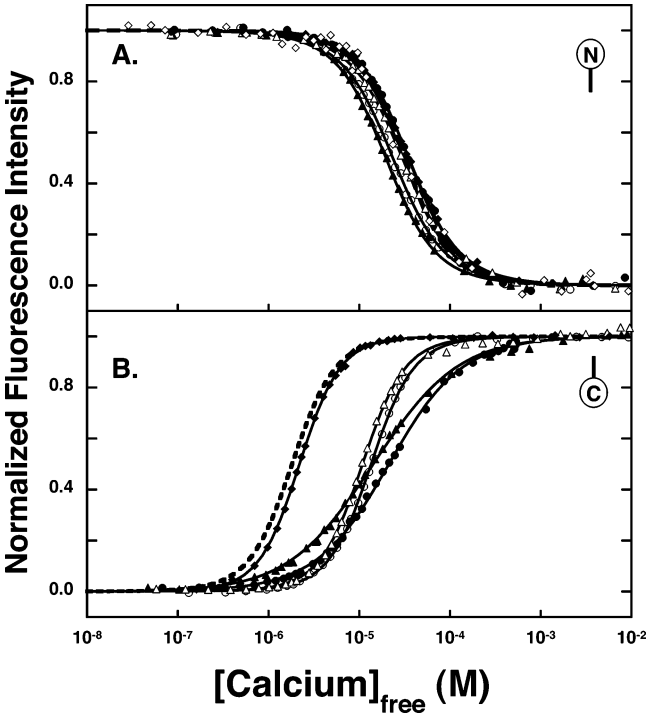

FIGURE 3: Calcium titrations of domain fragments of PCaM mutants. Normalized fluorescence intensity $[(f - f_{min})/(f_{max} - f_{min})]$ as a function of free calcium for titrations conducted in 50 mM HEPES, 100 mM KCl, 1 mM $MgCl_2$, 50 M EGTA, and 5 mM NTA at pH 7.4 and 22 °C. (A) N-domain fragments ($PCaM_{1-80}$) of six mutants defective in regulating calcium-dependent sodium-channel function: V35I/D50N (●), G40E (○), G40E/D50N (▲), D50G (△), E54K (◆), and G59S (◇). (B) C-domain fragments ($PCaM_{76-148}$) of five mutants defective in regulating calcium-dependent potassium-channel function: D95G (●), S101F (○), E104K (▲), H135R (△), and M145V (◆). Titrations shown are one representative trial of at least three replicates for each PCaM mutant sequence studied. In each panel, the solid black curve was simulated using the best-fit values resolved for the data set shown and the behavior of the corresponding wild-type fragment is represented by a black dashed curve.

was simulated using the best-fit values resolved from the data set shown. A titration of sites III and IV in the C-domain in $PCaM_{1-148}$ is shown as the dashed curve. The decrease in affinity of $PCaM_{76-148}$ (0.43 kcal/mol) relative to $PCaM_{1-148}$ is statistically significant and similar to that observed for a calcium-binding comparison of mammalian CaM_{76-148} to CaM_{1-148} (*17*).

Under-Reactive Mutants. Six PCaM mutants that affect the regulation of the calcium-dependent sodium current of *Paramecium* were studied. Five of these have modifications between sites I and II, while one (G59S) is modified in site II of the N-domain (see Figure 1). Titrations of $PCaM_{1-80}$ (Figure 3A) and $PCaM_{1-148}$ (Figure 4) containing these mutations were conducted to determine how their calcium-binding properties differed from those of wild-type PCaM. The results (Table 1) showed that the total free energy of calcium binding to sites I and II in all six of these mutants was similar to that of wild-type PCaM, whose behavior is represented by the dashed simulated titration in Figures 3 and 4. There were slightly greater differences observed among the $PCaM_{1-80}$ fragments of the mutants than among their corresponding full-length counterparts.

Two mutants showed a small but statistically significant decrease in free energy of calcium binding to sites I and II, as compared to wild-type sequences of both $PCaM_{1-80}$ and $PCaM_{1-148}$. Both contained the G40E mutation, located at the junction between the two EF-hands of the N-domain (Figure 1). This mutation alone caused the ΔG_2 of sites I and II in $PCaM_{1-148}$ to become more favorable by −0.25 kcal/mol and the corresponding sites in $PCaM_{1-80}$ to become more favorable by −0.36 kcal/mol (Table 1). The double mutation G40E/D50N also had a favorable effect on calcium binding. Relative to wild-type PCaM, the value of ΔG_2 for sites I and II was lowered by −0.41 kcal/mol in $PCaM_{1-148}$ and by −0.58 kcal/mol in $PCaM_{1-80}$. These differences exceeded the experimental standard deviations for the average values for three or more replicate titrations of these proteins.

A comparison of calcium affinities for sites I and II in $PCaM_{1-148}$ and $PCaM_{1-80}$ (Figure 5A) showed that, for the wild-type sequence and four of the under-reactive mutants, calcium binding to sites I and II in $PCaM_{1-80}$ was ∼0.2 kcal/mol less favorable than the same sites in $PCaM_{1-148}$. For the two G40E-containing mutants, there was no significant difference in the energies of calcium binding to sites I and II in $PCaM_{1-148}$ and $PCaM_{1-80}$ (i.e., the presence of the C-domain had no measurable effect).

In these under-reactive $PCaM_{1-148}$ mutants, the sequence of the C-domain is identical to that of wild-type $PCaM_{1-148}$. Calcium titrations of sites III and IV in these mutants (△ in Figure 4) were nearly identical to those of wild-type $PCaM_{1-148}$ (- - - in Figure 4). The free energies of calcium binding are given in Table 2. The largest differences were observed for E54K $PCaM_{1-148}$ ($\Delta\Delta G_2$ was 0.32 kcal/mol) and G59S $PCaM_{1-148}$ ($\Delta\Delta G_2$ was −0.32 kcal/mol). These differences were larger than the confidence intervals obtained in fits of individual titrations (<0.1 kcal/mol) and the standard deviation (<0.1 kcal/mol) computed when fits of three or more independent trials were averaged. Estimates of cooperative free energies of interaction (ΔG_c) between the paired sites in each domain according to eq 4 showed small differences.

Over-Reactive Mutants. All but one of the over-reactive mutants in *Paramecium* contains mutations within calcium-binding sites III and IV (Figure 1). The exception, M145V, is located outside of site IV, near the C-terminal residue (K148) of PCaM. Calcium titrations of mutant forms of $PCaM_{76-148}$ (Figure 3B) and $PCaM_{1-148}$ (Figure 6) were performed to determine how their calcium-binding properties differed from those of wild-type PCaM. The results showed a decrease in the calcium affinity of sites III and IV for all five mutants with an amino acid substitution within one of the sites, with the greatest decrease observed for E104K, which abolished any observable binding to site III at concentrations of calcium up to 2.42 mM (17.10 Ca^{2+}/CaM; data not shown). The slope of the titration of D95G was similar to that of E104K, but stoichiometric titrations (not shown) demonstrated that the C-domain of D95G bound 2 calcium ions. Therefore, the molecular basis for the change may be distinct. Titrations of calcium binding to sites III and IV in M145V were nearly identical to those of wild-type PCaM. A comparison of calcium affinities of these sites in $PCaM_{1-148}$ and $PCaM_{76-148}$ (Figure 5B) showed that, for wild-type PCaM and these over-reactive mutants, calcium

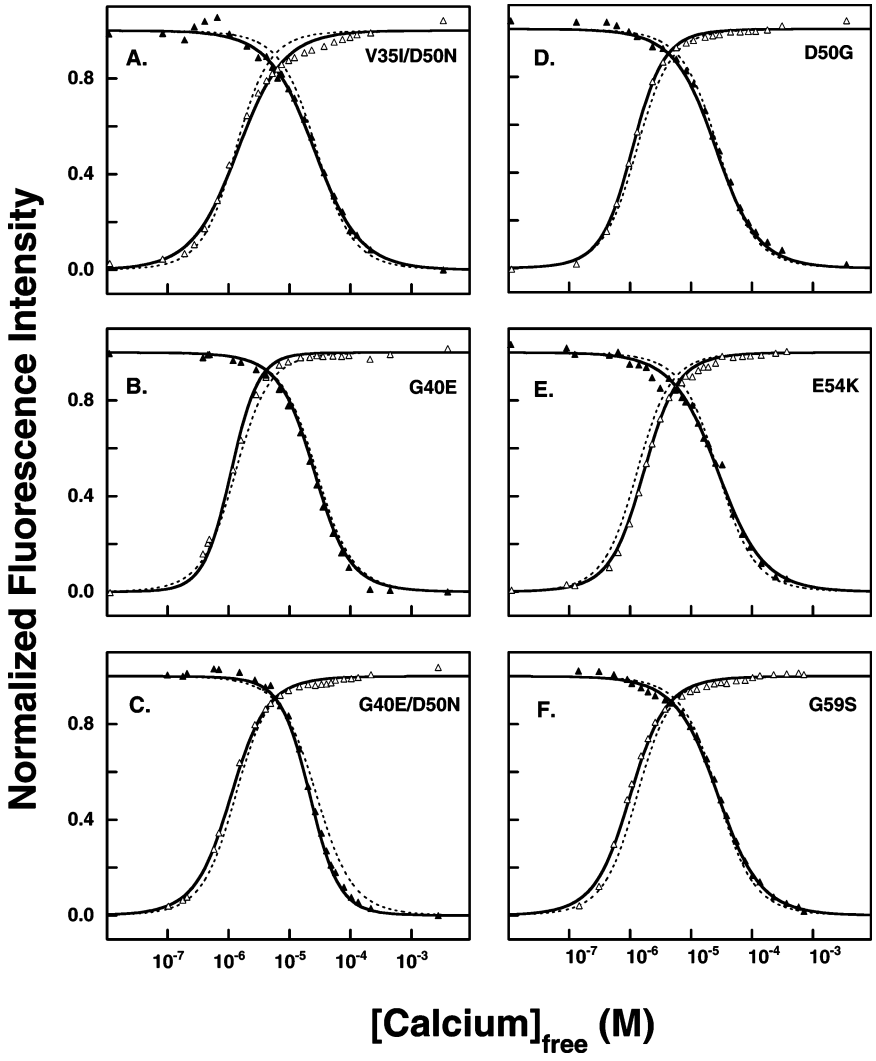

FIGURE 4: Calcium titrations of under-reactive PCaM mutants. The normalized fluorescence intensity $[(f - f_{min})/(f_{max} - f_{min})]$ for Phe (▲) and Tyr (△) is shown as a function of free calcium for six mutants defective in regulating calcium-dependent sodium-channel function. Titrations of (A) V35I/D50N$_{1-148}$, (B) G40E$_{1-148}$, (C) G40E/D50N$_{1-148}$, (D) D50G$_{1-148}$, (E) E54K$_{1-148}$, and (F) G59S$_{1-148}$ PCaM were conducted in 50 mM HEPES, 100 mM KCl, 1 mM $MgCl_2$, 50 μM EGTA, and 5 mM NTA at pH 7.4 and 22 °C. The solid black curve was simulated using the best-fit values resolved for the data set shown, and the dashed line in each panel represents the behavior of wild-type PCaM$_{1-148}$. Titrations shown are one representative trial of at least three replicates for each PCaM mutant sequence studied.

binding to sites III and IV in PCaM$_{76-148}$ was ~0.5 kcal/mol less favorable than to the same sites in PCaM$_{1-148}$, as had been observed for wild-type PCaM (Figure 2C).

In this set of five over-reactive mutants, the N-domain sequence is identical to that of wild-type PCaM$_{1-148}$. Stoichiometric titrations (not shown) demonstrated that the fractional occupancy of calcium-binding sites I and II was linearly proportional to the decrease in Phe fluorescence intensity. Thus, the fluorescence signal of the three Phe residues in the C domain made no contribution to the calcium-dependent Phe fluorescence signal. To evaluate the effects of mutations on the calcium affinity of sites I and II, it was necessary to determine whether the Phe residues in the C-domain of mutant PCaM sequences behaved in the same way as those in wild-type PCaM.

To test this, calcium-dependent changes in Phe fluorescence of the isolated mutant C-domain fragments (PCaM$_{76-148}$) were measured. For D95G, E104K, H135R, and M145V, the net calcium-induced change in steady-state fluorescence intensity of the Phe (250/280) signal of PCaM$_{76-148}$ was <4% of that observed for the corresponding mutant form of PCaM$_{1-148}$ (data not shown). Therefore, for these four mutants, the contribution of fluorescence intensity arising from calcium binding to the C-domain was considered negligible and the decrease in signal from PCaM$_{1-148}$ was interpreted as reflecting changes in the occupancy of sites I and II. The free energies of calcium binding to sites I and II were resolved using eq 2a. In PCaM$_{1-148}$, mutations D95G and H135R did not significantly alter the calcium-binding properties of the N-domain (see Table 1). The mutation M145V ($\Delta\Delta G_2 = -0.32$) caused a small increase in affinity of sites I and II, while the mutation E104K ($\Delta\Delta G_2 = -0.82$) caused a large increase in affinity. The effect of the fifth over-reactive mutation, S101F, on calcium binding required an analysis of the spectroscopic contribution of the newly introduced F101.

Phe Intensity of S101F PCaM. Of the 11 mutants studied here, only 1 (S101F) changed the composition of aromatic groups in PCaM. The addition of a Phe residue in site III caused a calcium-dependent decrease in the raw (unnormalized) Phe fluorescence signal of S101F PCaM$_{76-148}$ that was approximately one-quarter (22.5 ± 1.7%) of the

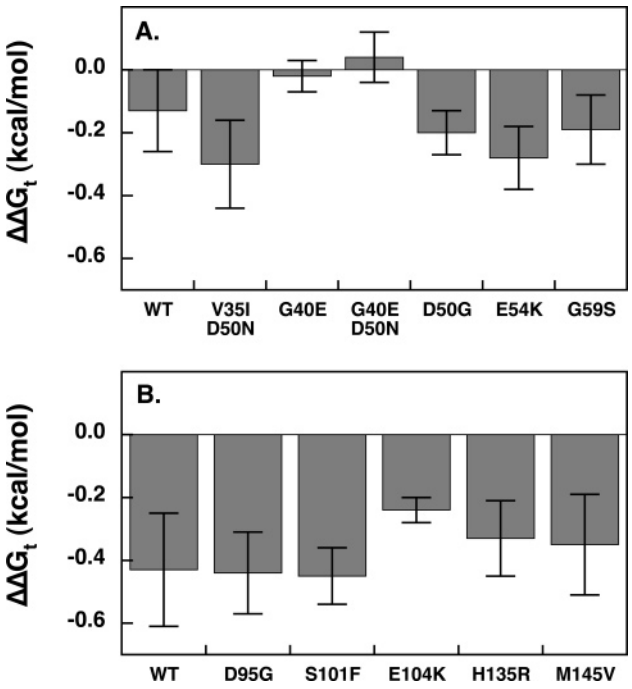

FIGURE 5: Differences in the free energies of calcium binding to domain fragments and full-length mutant PCaM molecules. A bar graph representation of the differences between the total free energy of calcium binding to (A) sites I and II of wild-type and mutant $PCaM_{1-148}$ and $PCaM_{1-80}$ and (B) sites III and IV of wild-type and mutant $PCaM_{1-148}$ and $PCaM_{76-148}$. For all mutants, except E104K, this reflected differences in ΔG_2 (see $\Delta\Delta G_2$ in Tables 1 and 2). E104K binds only 1 Ca^{2+} to the C-domain, and $\Delta\Delta G_1$ rather than $\Delta\Delta G_2$ differences are reported. Errors were propagated from the full-length and fragment data.

decrease in the signal observed for S101F $PCaM_{1-148}$ (see the Materials and Methods). This indicated that the total change in the Phe fluorescence signal observed in a titration of S101F $PCaM_{1-148}$ contained contributions from calcium binding to sites in both of the domains, rather than from the N-domain alone. Therefore, the calcium-dependent decrease in Phe fluorescence intensity of S101F $PCaM_{1-148}$ was analyzed according to eq 5. The free energies of calcium binding to sites I and II resolved from this analysis of the total change in Phe fluorescence of S101F $PCaM_{1-148}$ revealed that this mutation in the C-domain caused a slight decrease in calcium affinity of the sites ($\Delta\Delta G_2$ of 0.22 kcal/mol) in the N-domain (see Table 1) relative to the values determined for wild-type PCaM.

Model-Dependent Analysis of D95G Assuming Independent Sites. The free energy of cooperativity (ΔG_c) between the paired sites (I and II or III and IV) was estimated by assuming a model in which each of the sites within a domain had equal intrinsic calcium affinity, an assumption supported but not proven by NMR studies of PCaM (*2*). Wild-type $PCaM_{1-148}$ had a cooperative binding energy of −1.21 kcal/mol for sites III and IV, indicating favorable site−site interactions. In contrast, the calculated values of ΔG_c for sites III and IV in the over-reactive mutant D95G suggested slightly anti-cooperative calcium binding in D95G $PCaM_{1-148}$ (ΔG_c of +0.31 kcal/mol) and essentially independent binding in D95G $PCaM_{76-148}$ (ΔG_c of −0.09 kcal/mol).

A macroscopic binding isotherm that is apparently anti-cooperative may also arise from the binding of a ligand to two sites that are nonequivalent and independent. Thus, to determine the extent of difference possible between the intrinsic affinity of sites III and IV in the D95G C-domain, the isotherms were analyzed using a model in which the two sites were treated as independent ($k_c = 1$, and $\Delta G_c = 0$ kcal/mol) but were allowed to have different intrinsic binding affinities ($k_1 \neq k_2$). With this assumption, individual free energies of binding calcium to site III or IV could be estimated from the model-independent determination of ΔG_2 using eqs 7 and 8. For D95G $PCaM_{1-148}$, the estimated intrinsic free energies (corresponding to k_1 and k_2) were −6.07 and −6.95 kcal/mol, indicating a difference of 0.88 kcal/mol between the two sites. These individual-site values represent the largest possible difference in intrinsic free energies between the two sites that is also consistent with the classical average titration determined experimentally (see Figure 3 in ref *27* for a similar case). The corresponding independent individual-site isotherms are shown as solid curves in Figure 6F, with a simulated average degree of saturation shown as a dashed curve. Experimental studies in which it was possible to to distinguish the saturation of site III from site IV would be required to determine whether intrinsic site differences, changes in cooperativity, or both contributed to the observed average fractional saturation.

DISCUSSION

Calcium-binding energetics of 11 viable mutants of PCaM identified by their effects on ion-channel regulation and ensuing irregular stimulus-avoidance behavior of *Paramecia* were studied by observing calcium-dependent decreases in intrinsic Phe fluorescence that indicated the occupancy of sites I and II in the N-domain and increases in intrinsic Tyr fluorescence that indicated the occupancy of sites III and IV in the C-domain. Possible effects of the mutations on interdomain interactions were explored by comparing the calcium-binding energetics to sites in the N- and C-domain fragments ($PCaM_{1-80}$ and $PCaM_{76-148}$) to the corresponding sites in full-length PCaM ($PCaM_{1-148}$).

Under-Reactive (N-Domain) Mutants. Although one of the six under-reactive mutants studied contained a substitution within site II (G59S), all six of these mutants bound calcium in both domains in a manner very similar to that of wild-type PCaM under the conditions of this study (Figure 4). The largest differences in ΔG_2 observed for sites I and II in under-reactive mutants of $PCaM_{1-148}$ were −0.25 kcal/mol for G40E and −0.41 kcal/mol for G40E/D50N. The effects of these mutations on calcium binding to sites I and II were conserved in studies of the isolated mutant N-domain fragments terminating at residue 80 (see Table 1). It had been shown previously that fragments of wild-type PCaM terminating at residue 77, 78, 79, or 80 have free energies of calcium binding that are similar to that observed for sites I and II in $PCaM_{1-148}$ (*25*). In this study, the behavior of sites I and II in all of the under-reactive mutant $PCaM_{1-80}$ closely paralleled the corresponding sites in $PCaM_{1-148}$ (see Figure 5A). The absence of an effect of these mutations on the C-domain agreed with a prior study that was conducted without magnesium and was restricted to observing only sites III and IV (*35*). We conclude that these mutations do not disrupt the biophysical properties that are necessary for maintaining the affinities of sites I and II in the domain fragment, even though they may change other properties as was observed

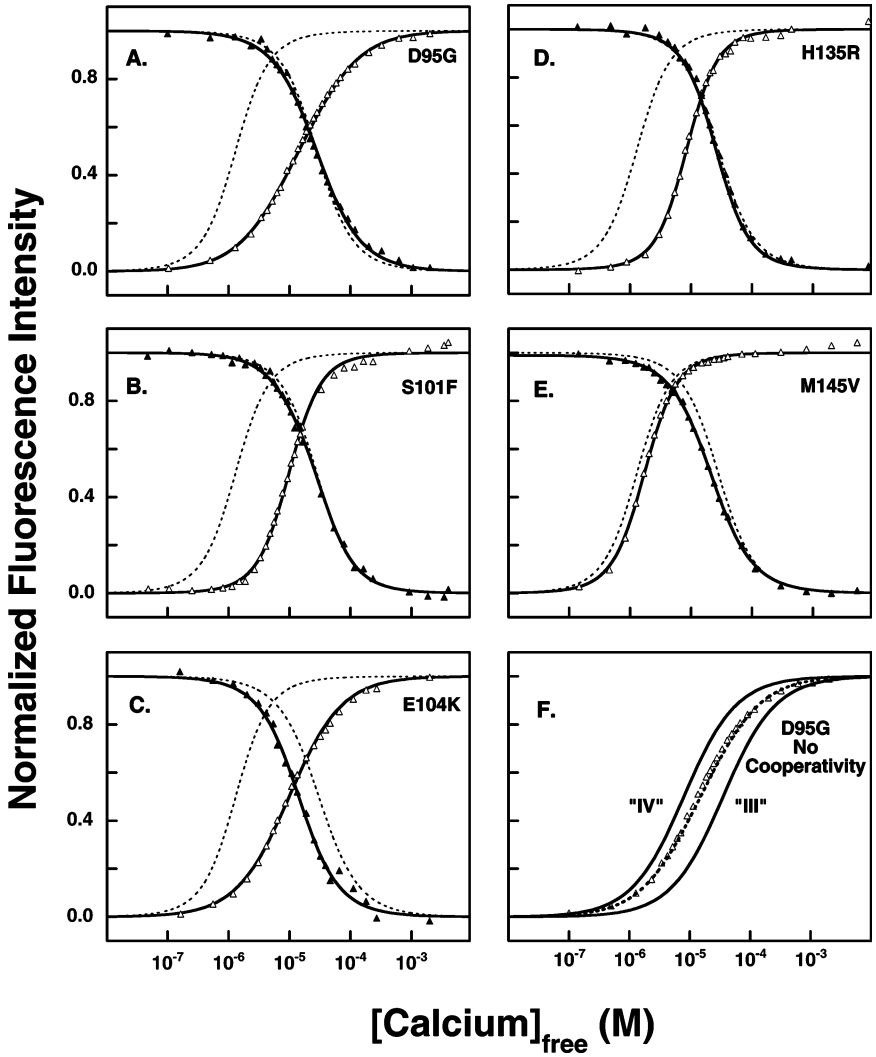

FIGURE 6: Calcium titrations of over-reactive PCaM mutants. Normalized measurements of fluorescence intensity $[(f - f_{min})/(f_{max} - f_{min})]$ for Phe (▲) and Tyr (△) are shown as a function of free calcium for five mutants defective in regulating calcium-dependent potassium-channel function. Titrations of (A) D95G, (B) S101F, (C) E104K, (D) H135R, and (E) M145V $PCaM_{1-148}$ were conducted in 50 mM HEPES, 100 mM KCl, 1 mM $MgCl_2$, 50 μM EGTA, and 5 mM NTA at pH 7.4 and 22 °C. The solid (—) line indicates the fit for the individual representative titration shown, and the dashed line (- - -) in each panel represents a simulation of the behavior of wild-type $PCaM_{1-148}$. Titrations shown are one representative trial of at least three replicates for each $PCaM_{1-148}$ mutant sequence studied. (F) Fractional saturation (—; eq 2b) for two sites of the $D95G_{1-148}$ C-domain simulated by assuming that calcium binding is noncooperative ($k_c = 1$). The average fractional saturation of the domain (eq 9) is indicated by a dashed line that overlays the experimental data (△).

in studies of thermal stability and Stokes radius of shorter fragments [$PCaM_{1-75}$ (*29*)] of these mutants.

Given that the substitutions found in the under-reactive mutants had little effect on intrinsic calcium-binding properties but are known to affect the calcium-dependent regulation of ion channels, we conclude that the association with the target proteins must disrupt normal calcium-induced conformational switching. Thus, it is likely that (a) the amino acids at these positions are highly conserved throughout evolution and (b) the substitutions disrupt an energetically favorable contact between CaM and one or more of its target proteins.

We explored these ideas by comparing CaM sequences from 50 eukaryotes, including plants, invertebrates, and vertebrates (see Figure 2 in ref *25*). This alignment showed that all of the residues from 32 to 55 (i.e., those between sites I and II; Figure 1B) are almost completely conserved with a substitution entropy (as described in ref *36*) of 0 for each residue except for two positions, Q49 and N53, each of which had a substitution entropy of 0.097 (still highly conserved). This degree of sequence identity highlights the importance of this region of CaM for its physiological function. It may be that the PCaM mutations discovered in this region occur at the few positions that allow the organism to remain viable, although crippled, and that mutations at other positions between sites I and II were lethal.

The positions of V35, G40, E54, D50, and G59 are highlighted in a structure resolved for CaM bound to a peptide from CaMKII [Protein Data Bank (PDB) 1CDM (*13*)], in which only V35 made contacts with the peptide (Figure 7A), and in a structure of CaM bound to the SK channel [PDB 1G4Y (*5*)], in which V35, D50, and E54 made contacts with a peptide fragment of the SK channel peptide (Figure 7B). To investigate the importance of the positions of under-reactive mutants to the interface between CaM and its targets, we used the Contacts of Structural Units (CSU) software (*37*) to determine the frequency at which each residue in wild-type CaM was within 4.5 Å of a residue in 15 structures of CaM−target co-complexes available in the PDB (parts C and D of Figure 7). Of the five positions found

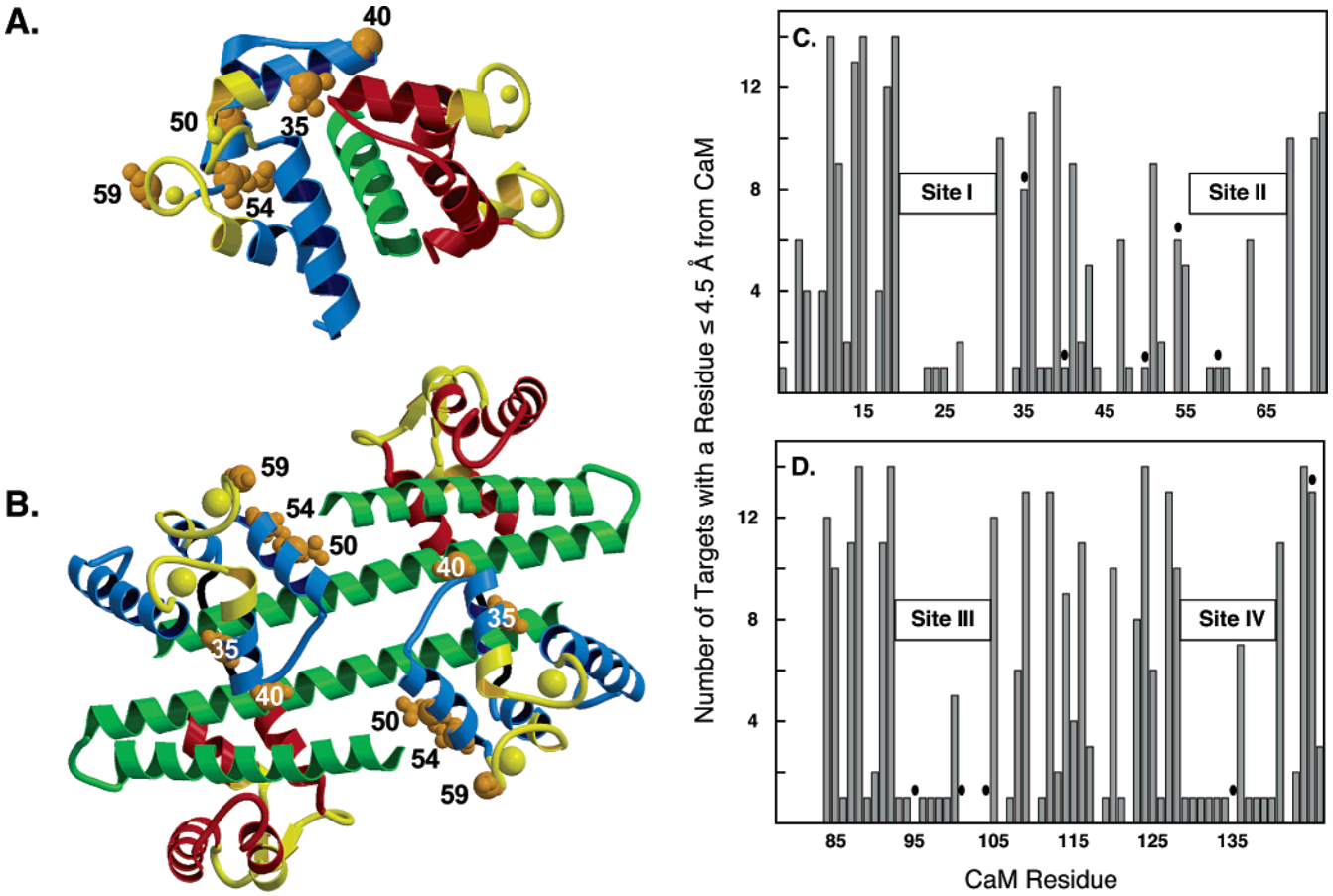

FIGURE 7: Ribbon diagram of $(Ca^{2+})_4$-CaM bound to a peptide (green) representing the CaM-binding domain of (A) Ca^{2+}-CaM-dependent protein kinase IIα [CaMKII, PDB 1CDM (*13*)] and (B) the SK channel [PDB 1G4Y (*5*)]. Positions of the under-reactive PCaM mutations are highlighted by space-filling models of the residues (orange). In CaM, residues 1−75 are blue, residues 76−80 are black, and residues 81−148 and calcium-binding sites are yellow. Ribbon drawings were created using MOLSCRIPT (*53*) and Raster3D (*54*). A CSU (*37*) analysis of the residues in the N-domain (C) and C-domain (D) of wild-type CaM that are ≤4.5 Å of residues in 15 CaM/target co-complexes available in the PDB. Only residues common in all 15 structures are shown (residues 5−72 in A and residues 84−146 in B). Those compared were smMLCK [PDB 1CDL (*11*)], skMLCK [PDB 2BBM (*55*)], CaMKI [PDB 1MXE (*56*)], CaMKIIα [PDB 1CDM (*13*)], CaM kinase kinase [PDB 1IQ5 (*57*) and 1CKK (*58*)], SK channel [PDB 1G4Y (*5*)], MARCKs [PDB 1IWQ (*59*)], endothelial nitric oxide synthase [PDB 1NIW (*60*)], anthrax edema factor [PDB 1K90 (*6*)], myristoylated CAP-23/NAP-22 [PDB 1L7Z (*61*)], olfactory CNG channel [PDB 1SY9 (*62*)], $CaV_{1.2}$IQ [PDB 2BE6 (*63*)], myosin VI [PDB 2BKH (*64*)], and glutamate decarboxylase [PDB 1NWD, chain B (*65*)]. Positions of the mutations in the under- and over-reactive mutants are highlighted with a black dot.

mutated in the under-reactive forms of PCaM, V35 and E54 made contacts with the largest number of targets (V35 was within 4.5 Å of a residue in 8 (53%) of the 15 targets studied, and E54 was within 4.5 Å of a residue in 6 (40%) of the 15 targets studied). While G40 had a contact in only 1 of these structures (CaM/anthrax edema factor peptide; PDB 1K90), which might be expected given the lack of a bulky side chain at this position, the neighboring residue L39 had contacts in 80% and Q41 had contacts in 60% of the 15 structures studied. This is consistent with the hypothesis that the physiologically identified substitution of glutamate for glycine at position 40 might disrupt a patch of favorable contacts. Similarly, although D50 had a contact in only 1 of these structures (CaM/SK channel peptide; PDB 1G4Y), its neighbor M51 had contacts in 60% of the 15 structures studied. The residue G59 within site II was the only residue among the five mutated in the under-reactive forms of PCaM that made a contact in only 1 structure (CaM/myosin VI; PDB 2BKH) and had neighbors that also only contacted ≤1 structure of a CaM−target complex (also in PDB 2BKH). In general, very few contacts were observed for most residues located within calcium-binding sites I and II (see Figure 7C).

This analysis demonstrates that the under-reactive mutations of PCaM may cause some local perturbations but most likely have long-range, allosteric effects on the functional properties of PCaM in a complex with a target. A model of the effect that these mutants may have on sodium-channel function in *Paramecia* is presented in Figure 8A and is similar to the interactions observed between CaM and the *N*-methyl-D-aspartate-type (NMDA) glutamate receptors (*38*). In this model, CaM is pre-associated with the channel in the absence of calcium via its C-terminal domain and calcium binding to sites I and II in the N-domain of CaM is required for the association of that domain and channel activation. The under-reactive mutants with defective sodium-channel regulation in *Paramecia* may associate with the channel in the absence of calcium and bind calcium like the wild-type but cannot undergo the conformational changes required for association of N-domain and channel activation.

Over-Reactive (C-Domain) Mutants. In the 12-residue calcium-binding loops of each EF-hand in CaM, amino acids at positions 1, 3, 5, 7, 9, and 12 coordinate calcium, some via carboxyl groups and others via their backbone carbonyl group (*39*). The importance of residues in these positions

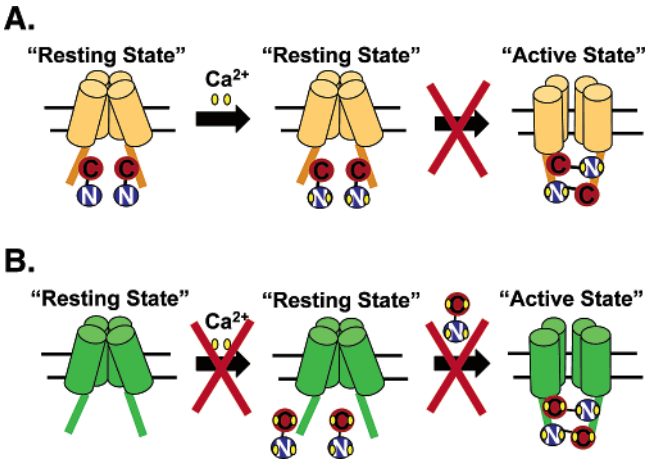

FIGURE 8: Models for compromised regulation of (A) sodium-channel activity by the under-reactive mutants and (B) potassium-channel regulation by the over-reactive mutants. In model A, the C-domain of CaM is pre-associated with the channel and calcium is required for N-domain association and channel activation. Mutations in the under-reactive mutants most likely disrupt allosteric effects necessary for N-domain association. In model B, calcium is required for association and activation. Mutations (except M145V) in the over-reactive mutants alter calcium binding and consequently disrupt target association.

for tuning the affinities of these sites has been demonstrated (*40*). Of the five over-reactive mutants studied, four have mutations in these positions (the exception is M145V; Figure 1B). Therefore, the observed diminution of calcium affinity of sites III and IV in these mutants was expected. The most dramatic decrease in affinity was observed for E104K, which abolished binding to site III. In that mutant, the free energy of calcium binding at the remaining site (site IV) was similar to that of ΔG_1 for wild-type $PCaM_{76-148}$.

In wild-type PCaM, the difference in the median ligand activities of the N- and C-domains is a factor of 22. This separation leads to a highly populated intermediate state in which both sites of the C-domain are occupied, while the N-domain sites are vacant. The significant decrease in the calcium affinity of the C-domain of the over-reactive mutants reduced the separation between the calcium-binding affinities of the N- and C-domains. Consequently, contrary to wild-type PCaM, the intermediate in which the C-domain is calcium-saturated and the N-domain is vacant is not populated to a significant level. If such an intermediate is important in the regulation of the calcium-activated potassium channels, its loss could explain the dysfunctional regulation of ion channels.

In addition to abolishing calcium binding to site III, the E104K mutation also caused an increase in affinity (by ~1 kcal/mol) of sites I and II in the N-domain of $E104K_{1-148}$. The effect of a mutation in the C-domain improving the affinity of the N-domain was observed for a site IV knockout mutation (E140Q) in mammalian CaM in which sites I and II were half-saturated at a calcium level lower than that required for the same sites in wild-type CaM (*41*) and studies of a series of site knockouts of *Drosophila* CaM (DCaM) (*42*). These results and others (*43*) illustrate that coupling within the C-domain of CaM affects interdomain communication; however, the mechanism by which this occurs remains unclear.

All of the mutations in sites III and IV lowered the calcium affinity of the C-domain. The mutation D95G also caused a loss of cooperativity (in $PCaM_{76-148}$) or apparent anti-cooperativity (in $PCaM_{1-148}$) between sites III and IV, consistent with what was observed when D95 was mutated to asparagine in mammalian CaM (*44*). It is possible that the effect of this residue is primarily to disrupt structural coupling between the paired helix−loop−helix units in the C-domain of PCaM. However, as shown in Figure 6F, the macroscopic isotherm (reflecting average occupancy of the two sites) is very well-represented by the sum of isotherms for sites that bind calcium independently but with different affinities, and this interpretation seems consistent with the mutation of only one site. The major effect of this mutation is probably to lower the midpoint of the titration, but site differences could play a role in the dynamics of association and/or activation of targets of CaM.

Unlike the other over-reactive mutants, all sites of M145V $PCaM_{1-148}$ and both sites in M145V $PCaM_{76-148}$ have calcium-binding properties similar to those of wild-type PCaM. It is likely that this mutation primarily affects the process of association or activation of a target, but it might also affect calcium-binding properties of PCaM bound to a target. It is well-established that methionine residues within the hydrophobic pockets of CaM are important in binding targets (*18*, *19*). Residue M145 has contacts in 13 of the 15 target−CaM co-complex structures in the PDB mentioned previously as analyzed by CSU (*37*), while the residues changed in the other over-reactive mutants did not have any contacts in these structures (Figure 7B). Studies of oxidation properties of the vicinal Met residues showed that target-binding properties are very sensitive to the integrity of M145 (*45*−*47*).

The effects of mutations on calcium binding to $PCaM_{1-148}$ were conserved in studies of the isolated C-domain fragments beginning at residue 76 (see Table 1). The slight increase in affinity (~0.5 kcal/mol) of sites III and IV in wild-type $PCaM_{1-148}$ relative to sites III and IV in wild-type $PCaM_{76-148}$ (see Figure 5B) was similar to that observed for mammalian CaM (*17*) and was also observed for each of the five over-reactive mutants. This indicates that the tertiary structure of an N-domain with wild-type sequence favorably affects the affinity of the calcium-binding sites in the C-domain. In keeping with the effects of the E104K mutation on the N-domain, it provides additional evidence for distributed inter-domain interactions, despite the lack of any close, persistent contacts in solution such as that which would be monitored in NMR NOE experiments (*2*).

In the genetic screen that yielded these altered forms of PCaM, mutations in the C-domain of PCaM caused a lengthening of the interval of avoidance behavior in response to various stimuli, as well as a decrease in the calcium-activated potassium current relative to wild-type *Paramecium* (*14*). If calcium binding to the C-domain of PCaM is necessary and sufficient to trigger normal regulatory behavior that would allow the organism to resume random sampling of its environment, then lowered calcium affinity would raise the effective concentration of cellular calcium required to saturate these mutants of PCaM. If, in turn, calcium saturation is required for the association of CaM with the ion channel and subsequent termination of the avoidance response, then a decrease in calcium affinity would extend the duration of the calcium influx required to change channel behavior. In that case, the free energies of calcium binding measured in

this study may directly address the step in the physiological pathway disrupted by these mutations. A model for this mechanism is shown in Figure 8B.

SUMMARY

The linkage between calcium binding to CaM and the association with and activation of ion channels by CaM is a broadening area of interest and is being explored very successfully by making site-knockout mutants of CaM (*48*−*51*). However, by studying two classes of viable mutants of PCaM, we have shown that mutations may be deleterious without affecting intrinsic calcium-binding properties. Whether these are changed in the context of CaM bound to the *Paramecium* channel proteins awaits further investigation. However, given that the sequences of *Paramecium* and mammalian CaM are 88% identical, we believe these two classes of mutants will provide valuable probes of other CaM−target interactions. Further investigation into the target-linked conformational changes of these mutants and their energetics of binding to multiple targets will be necessary to understand the linked effects of these positions in channel regulation. However, these studies lay a foundation for elucidating the mechanism by which the highly homologous domains of CaM differentially regulate multiple classes of target proteins.

ACKNOWLEDGMENT

We thank C. Kung and K.-Y. Ling (University of Wisconsin−Madison) for sharing overexpression vectors for all PCaM sequences used in these studies, L. Faga for subcloning the mutant PCaM sequences into pT7-7, other members of the Shea laboratory for purification of some of the protein samples used in this study, and L. Teesch and E. Rus for amino acid analysis (Molecular Analysis Facility, University of Iowa College of Medicine).

REFERENCES

1. Seamon, K. B. (1980) Calcium- and magnesium-dependent conformational states of calmodulin as determined by nuclear magnetic resonance, *Biochemistry 19*, 207−215.
2. Jaren, O. R., Kranz, J. K., Sorensen, B. R., Wand, A. J., and Shea, M. A. (2001) Calcium-induced conformational switching of *Paramecium* calmodulin: Changes in the protein backbone observed by heteronuclear NMR studies, *Biochemistry 41*, 14158−14166.
3. LaPorte, D. C., Wierman, B. M., and Storm, D. R. (1980) Calcium-induced exposure of a hydrophobic surface on calmodulin, *Biochemistry 19*, 3814−3819.
4. Schumacher, M. A., Crum, M., and Miller, M. C. (2004) Crystal structures of apocalmodulin and an apocalmodulin/SK potassium channel gating domain complex, *Structure 12*, 849−860.
5. Schumacher, M. A., Rivard, A. F., Bachinger, H. P., and Adelman, J. P. (2001) Structure of the gating domain of a Ca^{2+}-activated K^+ channel complexed with Ca^{2+}/calmodulin, *Nature 410*, 1120−1124.
6. Drum, C. L., Yan, S., Bard, J., Shen, Y., Lu, D., Soelaiman, S., Grabarek, Z., Bohm, A., and Tang, W. (2002) Structural basis for the activation of anthrax adenylyl cyclase exotoxin by calmodulin, *Nature 415*, 396−402.
7. Bähler, M., and Rhoads, A. (2002) Calmodulin signaling via the IQ motif, *FEBS Lett. 513*, 107−113.
8. Urbauer, J. L., Short, J. H., Dow, L. K., and Wand, A. J. (1995) Structural analysis of a novel interaction by calmodulin: High affinity binding of a peptide in the absence of calcium, *Biochemistry 34*, 8099−8109.
9. Jurado, L. A., Chockalingam, P. S., and Jarrett, H. W. (1999) Apocalmodulin, *Physiol. Rev. 79*, 661−682.
10. Saimi, Y., and Kung, C. (2002) Calmodulin as an ion-channel subunit, *Annu. Rev. Physiol. 64*, 289−311.
11. Meador, W. E., Means, A. R., and Quiocho, F. A. (1992) Target enzyme recognition by calmodulin: 2.4 Å structure of a calmodulin−peptide complex, *Science 257*, 1251−1255.
12. Ikura, M., Barbato, G., Klee, C. B., and Bax, A. (1992) Solution structure of calmodulin and its complex with a myosin light chain kinase fragment, *Cell Calcium 13*, 391−400.
13. Meador, W. E., Means, A. R., and Quiocho, F. A. (1993) Modulation of calmodulin plasticity in molecular recognition on the basis of X-ray structures, *Science 262*, 1718−1721.
14. Kung, C., Preston, R. R., Maley, M. E., Ling, K.-Y., Kanabrocki, J. A., Seavey, B. R., and Saimi, Y. (1992) *In vivo Paramecium* mutants show that calmodulin orchestrates membrane responses to stimuli, *Cell Calcium 13*, 413−425.
15. Pedigo, S., and Shea, M. A. (1995) Quantitative endoproteinase GluC footprinting of cooperative Ca^{2+} binding to calmodulin: Proteolytic susceptibility of E31 and E87 indicates interdomain interactions, *Biochemistry 34*, 1179−1196.
16. Shea, M. A., Sorensen, B. R., Pedigo, S., and Verhoeven, A. (2000) Proteolytic footprinting titrations for estimating ligand-binding constants and detecting pathways of conformational switching of calmodulin, *Methods Enzymol. 323*, 254−301.
17. Sorensen, B. R., and Shea, M. A. (1998) Interactions between domains of apo calmodulin alter calcium binding and stability, *Biochemistry 37*, 4244−4253.
18. O'Neil, K. T., and DeGrado, W. F. (1990) How calmodulin binds its targets: Sequence independent recognition of amphiphilic α-helices, *Trends Biochem. Sci. 15*, 59−64.
19. Crivici, A., and Ikura, M. (1995) Molecular and structural basis of target recognition by calmodulin, *Annu. Rev. Biophys. Biomol. Struct. 24*, 85−116.
20. VanScyoc, W. S., Sorensen, B. R., Rusinova, E., Laws, W. R., Ross, J. B., and Shea, M. A. (2002) Calcium binding to calmodulin mutants monitored by domain-specific intrinsic phenylalanine and tyrosine fluorescence, *Biophys. J. 83*, 2767−2780.
21. Studier, F. W., Rosenberg, A. H., Dunn, J. J., and Dubendorff, J. W. (1990) Use of T7 RNA polymerase to direct expression of cloned genes, *Methods Enzymol. 185*, 60−89.
22. Tabor, S., and Richardson, C. C. (1985) A bacteriophage T7 RNA polymerase/promoter system for controlled exclusive expression of specific genes, *Proc. Natl. Acad. Sci. U.S.A. 82*, 1074−1078.
23. Putkey, J. A., Slaughter, G. R., and Means, A. R. (1985) Bacterial expression and characterization of proteins derived from the chicken calmodulin cDNA and a calmodulin processed gene, *J. Biol. Chem. 260*, 4704−4712.
24. Newman, R. Roles of calmodulin domains in allosteric regulation of the ryanodine receptor type 1, Ph.D. Dissertation, University of Iowa, Iowa City, IA, 2006.
25. Faga, L. A., Sorensen, B. R., VanScyoc, W. S., and Shea, M. A. (2003) Basic interdomain boundary residues in calmodulin decrease calcium affinity of sites I and II by stabilizing helix−helix interactions, *Proteins: Struct., Funct., Genet. 50*, 381−391.
26. Starovasnik, M. A., Su, D. R., Beckingham, K., and Klevit, R. E. (1992) A series of point mutations reveal interactions between the calcium-binding sites of calmodulin, *Protein Sci. 1*, 245−253.
27. Ackers, G. K., Shea, M. A., and Smith, F. R. (1983) Free energy coupling within macromolecules: The chemical work of ligand binding at the individual sites in cooperative systems, *J. Mol. Biol. 170*, 223−242.
28. Adair, G. S. (1925) The osmotic pressure of haemoglobin in the absence of salts, *Proc. R. Soc. London, Ser. A 109*, 292−300.
29. VanScyoc, W. S., and Shea, M. A. (2001) Phenylalanine fluorescence studies of calcium binding to N-domain fragments of *Paramecium* calmodulin mutants show increased calcium affinity correlates with increased disorder, *Protein Sci. 10*, 1758−1768.
30. Maune, J. F., Klee, C. B., and Beckingham, K. (1992) Ca^{2+} binding and conformational change in two series of point mutations to the individual Ca^{2+}-binding sites of calmodulin, *J. Biol. Chem. 267*, 5286−5295.
31. Crouch, T. H., and Klee, C. B. (1980) Positive cooperative binding of calcium to bovine brain calmodulin, *Biochemistry 19*, 3692−3698.
32. Linse, S., Helmersson, A., and Forsén, S. (1991) Calcium binding to calmodulin and its globular domains, *J. Biol. Chem. 266*, 8050−8054.

33. Ababou, A., and Desjarlais, J. R. (2001) Solvation energetics and conformational change in EF-hand proteins, *Protein Sci. 10*, 301−312.
34. Masino, L., Martin, S. R., and Bayley, P. M. (2000) Ligand binding and thermodynamic stability of a multidomain protein, calmodulin, *Protein Sci. 9*, 1519−1529.
35. Jaren, O. R., Harmon, S., Chen, A. F., and Shea, M. A. (2000) *Paramecium* calmodulin mutants defective in ion channel regulation can bind calcium and undergo calcium-induced conformational switching, *Biochemistry 39*, 6881−6890.
36. Elcock, A. H. (2001) Prediction of functionally important residues based solely on the computed energetics of protein structure, *J. Mol. Biol. 312*, 885−896.
37. Sobolev, V., Sorokine, A., Prilusky, J., Abola, E. E., and Edelman, M. (1999) Automated analysis of interatomic contacts in proteins, *Bioinformatics 15*, 327−332.
38. Akyol, Z., Bartos, J. A., Merrill, M. A., Faga, L. A., Jaren, O. R., Shea, M. A., and Hell, J. W. (2004) Apo-calmodulin binds with its COOH-terminal domain to the *N*-methyl-D-aspartate receptor NR1 C0 region, *J. Biol. Chem. 279*, 2166−2175.
39. McPhalen, C. A., Strynadka, N. C. J., and James, M. N. G. (1991) Calcium-binding sites in proteins: A structural perspective, *Adv. Protein Chem. 42*, 77−144.
40. Reid, R. E., and Hodges, R. S. (1980) Co-operativity and calcium/magnesium binding to troponin C and muscle calcium binding parvalbumin: An hypothesis, *J. Theor. Biol. 84*, 401−444.
41. Shea, M. A., Verhoeven, A. S., and Pedigo, S. (1996) Calcium-induced interactions of calmodulin domains revealed by quantitative thrombin footprinting of Arg37 and Arg106, *Biochemistry 35*, 2943−2957.
42. Martin, S. R., Maune, J. F., Beckingham, K., and Bayley, P. M. (1992) Stopped-flow studies of calcium dissociation from calcium-binding-site mutants of *Drosophila melanogaster* calmodulin, *Eur. J. Biochem. 205*, 1107−1114.
43. Sun, H., Yin, D., Coffeen, L. A., Shea, M. A., and Squier, T. C. (2001) Mutation of Tyr138 disrupts the structural coupling between the opposing domains in vertebrate calmodulin, *Biochemistry 40*, 9605−9617.
44. Waltersson, Y., Linse, S., Brodin, P., and Grundström, T. (1993) Mutational effects on the cooperativity of Ca^{2+} binding in calmodulin, *Biochemistry 32*, 7866−7871.
45. Yao, Y., Yin, D., Jas, G. S., Kuczera, K., Williams, T. D., Schöneich, C., and Squier, T. C. (1996) Oxidative modification of a carboxyl-terminal vicinal methionine in calmodulin by hydrogen peroxide inhibits calmodulin-dependent activation of the plasma membrane Ca-ATPase, *Biochemistry 35*, 2767−2787.
46. Gao, J., Yin, D. H., Yao, Y., Sun, H., Qin, Z., Schöneich, C., Williams, T. D., and Squier, T. C. (1998) Loss of conformational stability in calmodulin upon methionine oxidation, *Biophys. J. 74*, 1115−1134.
47. Yin, D., Kuczera, K., and Squier, T. C. (2000) The sensitivity of carboxyl-terminal methionines in calmodulin isoforms to oxidation by H_2O_2 modulates the ability to activate the plasma membrane Ca-ATPase, *Chem. Res. Toxicol. 13*, 103−110.
48. Erickson, M. G., Liang, H., Mori, M. X., and Yue, D. T. (2003) FRET two-hybrid mapping reveals function and location of L-type Ca^{2+} channel CaM preassociation, *Neuron 39*, 97−107.
49. Kim, J., Ghosh, S., Nunziato, D. A., and Pitt, G. S. (2004) Identification of the components controlling inactivation of voltage-gated Ca^{2+} channels, *Neuron 41*, 745−754.
50. Xia, X. M., Fakler, B., Rivard, A., Wayman, G., Johnson-Pais, T., Keen, J. E., Ishii, T., Hirschberg, B., Bond, C. T., Lutsenko, S., Maylie, J., and Adelman, J. (1998) Mechanism of calcium gating in small-conductance calcium-activated potassium channels, *Nature 395*, 503−507.
51. Liang, H., DeMaria, C. D., Erickson, M. G., Mori, M. X., Alseikhan, B. A., and Yue, D. T. (2003) Unified mechanisms of Ca^{2+} regulation across the Ca^{2+} channel family, *Neuron 39*, 951−960.
52. Rao, S. T., Wu, S., Satyshur, K. A., Ling, K.-Y., Kung, C., and Sundaralingam, M. (1993) Structure of *Paramecium tetraurelia* calmodulin at 1.8 Å resolution, *Protein Sci. 2*, 436−447.
53. Kraulis, P. J. (1991) MOLSCRIPT: A program to produce both detailed and schematic plots of protein structures, *J. Appl. Crystallogr. 24*, 946−950.
54. Merritt, E. A., and Bacon, D. J. (1997) Raster3D: Photorealistic molecular graphics methods, *Methods Enzymol. 277*, 505−524.
55. Ikura, M., Clore, G. M., Gronenborn, A. M., Zhu, G., Klee, C. B., and Bax, A. (1992) Solution structure of a calmodulin−target peptide complex by multidimensional NMR, *Science 256*, 632−638.
56. Clapperton, J. A., Martin, S. R., Smerdon, S. J., Gamblin, S. J., and Bayley, P. M. (2002) Structure of the complex of calmodulin with the target sequences of calmodulin-dependent protein kinase I: Studies of the kinase activation mechanism, *Biochemistry 41*, 14669−14679.
57. Kurokawa, H., Osawa, M., Kurihara, H., Katayama, N., Tokumitsu, H., Swindells, M. B., Kainosho, M., and Ikura, M. (2001) Target-induced conformational adaptation of calmodulin revealed by the crystal structure of a complex with nematode Ca^{2+}/calmodulin-dependent kinase kinase peptide, *J. Mol. Biol. 312*, 59−68.
58. Osawa, M., Tokumitsu, H., Swindells, M. B., Kurihara, H., Orita, M., Shibanuma, T., Furuya, T., and Ikura, M. (1999) A novel target recognition revealed by calmodulin in complex with Ca^{2+}-calmodulin-dependent kinase kinase, *Nat. Struct. Biol. 6*, 819−824.
59. Yamauchi, E., Nakatsu, T., Matsubara, M., Kato, H., and Taniguchi, H. (2003) Crystal structure of a MARCKS peptide containing the calmodulin-binding domain complex with Ca^{2+}-calmodulin, *Nat. Struct. Biol. 10*, 226−231.
60. Aoyagi, M., Arvai, A. S., Tainer, J. A., and Getzoff, E. D. (2003) Structural basis for endothelial nitric oxide synthase binding to calmodulin, *EMBO J. 22*, 766−775.
61. Matsubara, M., Nakatsu, T., Kato, H., and Taniguchi, H. (2004) Crystal structure of a myristoylated CAP-23/NAP-22 N-terminal domain complexed with Ca^{2+}/calmodulin, *EMBO J. 23*, 712−718.
62. Contessa, G. M., Orsale, M., Melino, S., Torre, V., Paci, M., Desideri, A., and Cicero, D. O. (2005) Structure of calmodulin complexed with an olfactory CNG channel fragment and role of the central linker: Residual dipolar couplings to evaluate calmodulin binding modes outside the kinase family, *J. Biomol. NMR 31*, 185−199.
63. van Petegem, F., Chatelain, F. C., and Minor, D. L., Jr. (2005) Insights into voltage-gated calcium channel regulation from the structure of the $Ca_{(V)}1.2$ IQ domain-Ca^{2+}/calmodulin complex, *Nat. Struct. Mol. Biol. 12*, 1108−1115.
64. Opella, S. J., Marassi, F. M., Gesell, J. J., Valente, A. P., Kim, Y., Montal, M. O., and Montal, M. (1999) Structures of the M2 channel-lining segments from nicotinic acetylcholine and NMDA receptors by NMR spectroscopy, *Nat. Struct. Biol. 6*, 374−379.
65. Yap, K. L., Yuan, T., Mal, T. K., Vogel, H. J., and Ikura, M. (2003) Structural basis for simultaneous binding of two carboxy-terminal peptides of plant glutamate decarboxylase to calmodulin, *J. Mol. Biol. 328*, 193−204.

BI061134D